Redox Biology 32 (2020) 101496

Contents lists available at ScienceDirect

Redox Biology

journal homepage: www.elsevier.com/locate/redox

Peroxiredoxin 6 mediates acetaminophen-induced hepatocyte death through JNK activation

Dong Hun Lee[a,1], Young Suk Jung[b,1], Jaesuk Yun[c], Sang Bae Han[c], Yoon Seok Roh[c], Min Jong Song[d,**], Jin Tae Hong[c,*]

[a] Department of Biological Sciences, Chonnam National University, 77 Yongbong-ro, Buk-gu, Gwangju, 61186, Republic of Korea
[b] College of Pharmacy, Pusan National University, 2, Busandaehak-ro 63beon gil, Geumjeong-gu, Busan, 46241, Republic of Korea
[c] College of Pharmacy and Medical Research Center, Chungbuk National University, Osongsaengmyeong 1-ro 194-31, Osong-eup, Heungduk-gu, Cheongju, Chungbuk, 28160, Republic of Korea
[d] Department of Obstetrics and Gynecology, Daejeon St. Mary's Hospital, College of Medicine, The Catholic University of Korea, 64 Daeheung-ro, Jung-gu, Daejeon, 301-723, Republic of Korea

ARTICLE INFO

Keywords:
Peroxiredoxin 6
Acetaminophen
Calcium-independent phospholipase A_2
Lysophosphatidylcholine
c-Jun *N*-Terminal kinases

ABSTRACT

Acetaminophen (APAP) is one of the most frequently used drugs; however, its overdose leads to acute liver injury. Recently, studies have reported that the adduction of peroxiredoxin 6 (PRDX6), a member of the PRDX family of antioxidant enzymes, is associated with liver diseases. However, the role of PRDX6 in APAP-induced liver injury remains unclear. Here, we assessed both age-matched (about 12 weeks) PRDX6-overexpressing transgenic mice (PRDX6 mice) and wild type (WT) mice presenting acute liver injury induced by the intraperitoneal injection of APAP (500 mg/kg). Although PRDX6 is known as an antioxidant enzyme, PRDX6 mice unexpectedly demonstrated severe liver injury following APAP injection compared with WT mice. We observed that PRDX6 was hyperoxidized after APAP administration. Additionally, calcium-independent phospholipase A_2 (iPLA2) activity and lysophosphatidylcholine (LPC) levels were markedly elevated in PRDX6 mice following APAP administration. Moreover, APAP-induced JNK phosphorylation was considerably increased in the liver of PRDX6 mice. MJ33, an inhibitor of PRDX6, attenuated APAP-induced liver injury both in WT and PRDX6 mice. Notably, MJ33 reduced the APAP-induced increase in JNK activation, iPLA2 activity, and LPC levels. Although SP600125, a JNK inhibitor, abolished APAP-induced liver injury, it failed to affect the APAP-induced hyperoxidation of PRDX6, iPLA2 activity, and LPC levels. These results suggested that PRDX6 was converted to the hyperoxidized form by the APAP-induced high concentration of hydrogen peroxides. In the liver, hyperoxidized PRDX6 induced cellular toxicity via JNK activation by enhancing iPLA2 activity and LPC levels; this mechanism appears to be a one-way cascade.

1. Introduction

Acetaminophen (APAP) is a widely used antipyretic and analgesic drug at therapeutic levels but can cause severe acute liver injury following an overdose [1,2]. It is well established that APAP hepatotoxicity is initiated by the formation of *N*-acetyl-*p*-benzo-quinoneimine (NAPQI), a reactive metabolite generated by cytochrome p450 [3]. After an APAP overdose, excess NAPQI induces severe glutathione

Abbreviations: APAP, Acetaminophen; PRDX, peroxiredoxin; WT mice, wild type mice; PRDX6 mice, peroxiredoxin 6 overexpressing transgenic mice; NAPQI, *N*-acetyl-*p*-benzo-quinoneimine; iPLA2, calcium-independent phospholipase A_2; LPC, lysophosphatidylcholine; ROS, reactive oxygen species; JNK, c-Jun *N*-terminal kinases; AST, aspartate transaminase; ALT, alanine transaminase; GSH, Glutathione; GSSG, Oxidized Glutathione; CYP2E1, cytochrome p450 2E1; PRDX6-SO3, sulfonic acid formation of PRDX6

* Corresponding author. College of Pharmacy, Chungbuk National University, Osongsaengmyeong 1-ro 194-31, Osong-eup, Heungduk-gu, Cheongju, Chungbuk, 28160, Republic of Korea.
** Corresponding author. Department of Obstetrics and Gynecology, Daejeon St. Mary's Hospital, College of Medicine, The Catholic University of Korea, 64 Daeheung-ro, Jung-gu, Daejeon, 301-723, Republic of Korea.
E-mail addresses: leedonghun0154@gmail.com (D.H. Lee), youngjung@pusan.ac.kr (Y.S. Jung), jyun@chungbuk.ac.kr (J. Yun), shan@chungbuk.ac.kr (S.B. Han), ysroh@chungbuk.ac.kr (Y.S. Roh), bitsugar@catholic.ac.kr (M.J. Song), jinthong@chungbuk.ac.kr (J.T. Hong).
[1] These authors contributed equally to this work.

https://doi.org/10.1016/j.redox.2020.101496
Received 28 November 2019; Received in revised form 25 February 2020; Accepted 4 March 2020
Available online 08 March 2020

(GSH) depletion in mitochondria [4], inhibiting mitochondrial respiration [5] and leading to the formation of reactive oxygen species (ROS) [6]. The increased mitochondrial ROS activates the c-Jun *N*-terminal kinases (JNK) via several pathways. Then, the activated JNK translocates to the mitochondrial membrane and further enhances ROS production [7].

Peroxiredoxins (PRDXs) are antioxidant enzymes that control cytokine-induced peroxide levels and mediate signal transduction in mammalian cells. ROS can be scavenged by peroxidase, and PRDXs represent a superfamily of non-seleno peroxidases [8]. Many studies have reported that PRDXs are associated with various disease models involved in oxidative stress. PRDX2-deficient mice demonstrate increased susceptibility to lipopolysaccharide (LPS)-induced lethal shock, and an intravenous injection with the adenoviral PRDX2 gene rescued these mice from LPS-induced lethal shock by eliminating LPS-induced hydrogen peroxide [9]. In the adipose tissue, PRDX3 deficiency increases abnormal lipid accumulation owing to increased ROS production [10]. Additionally, HFD-induced hepatic steatosis and insulin resistance are prevented in PRDX4 transgenic mice following the amelioration of oxidative stress [11]. Unlike other members of the PRDXs family with two reactive cysteines, Prdx6 has a single redox-active cysteine residue. Roede et al. have reported that PRDX6 overexpression fails to prevent ethanol-induced oxidative stress in mice model [12]. PRDX6 demonstrates glutathione (GSH) peroxidase activity and its catalytic peroxidase mechanism is based on GSH instead of thioredoxin for physiological reduction [13]. However, PRDX6 also has calcium-independent phospholipase A_2 ($iPLA_2$) activity, which was elucidated by site-directed mutation analysis [14]. Thus, PRDX6 is a bifunctional enzyme with GSH peroxidase and $iPLA_2$ activities. Moreover, we previously reported that PRDX6 exacerbates collagen antibody-induced arthritis via JNK activation [15]. In the APAP-induced liver injury model, JNK, activated through several pathways and induced by ROS in the cytosol, translocates to the mitochondria and binds Sab (SH3 domain-binding protein), a scaffold protein on the outer mitochondrial membrane [16–18]. Translocation of the activated JNK to the mitochondria leads to further enhancement of mitochondrial ROS generation, mitochondrial permeabilization, and dysfunction [7]. Interestingly, the silencing or inhibition of JNK provides protection against APAP-induced liver injury, even in the presence of excessive mitochondrial GSH depletion and covalent binding [19,20]. Thus, JNK activation is a critical factor in APAP-induced liver injury.

In the present study, we investigated whether PRDX6 affects APAP-induced liver injury. Male mice demonstrate an enhanced susceptibility to APAP-induced hepatotoxicity than female mice [21], and Mohar et al. reported that the adduction of PRDX6 may be an important factor in APAP-induced glutamate-cysteine ligase modifier subunit (*Gclm*)-deficient mice exhibiting compromised GSH synthesis [22]. However, the function of PRDX6 in APAP-induced hepatotoxicity remains unclear. Therefore, we developed a model of APAP-induced acute liver injury in PRDX6 transgenic mice and investigated the role of PRDX6 in APAP-induced hepatic injury.

2. Materials and methods

2.1. Animals

The C57BL/6J-Tg (PRDX6) mice were purchased from the Jack-son Laboratory. The mice were housed and bred under specific pathogen free conditions at the Laboratory Animal Research Center of Chungbuk National University, Korea. The C57BL/6J wild type (WT) mice and PRDX6 mice, that were used, had matched ages (about 3 months old). To generate drug-induced acute liver injury model, mice were intraperitoneally (i.p.) pre-injected with JNK inhibitor, SP600125 (10 mg/kg, Sigma-Aldrich, St. Louis, MO, USA) or PRDX6 inhibitor, MJ33 (2.5 nmol/g, Santa Cruz Biotechnology, Dallas, Texas, USA) or not then after 3 h, i.p. injected with 500 mg/kg acetaminophen (APAP), and then mice were sacrificed at 6 h after APAP injection. All studies were approved by and performed according to the ethical guidelines by the Chungbuk National University Animal Care Committee (CBNUA-1073-17-01).

2.2. The serum chemistry measurements

Mice were anesthetized with an overdose of pentobarbital (100 mg/kg) and blood was taken by heart puncture. Serum levels of aspartate transaminase (AST) and alanine transaminase (ALT) in the liver of mice were measured by using an automated analyzer (7080, Hitachi Ltd., Japan) at laboratory animal research center in Chungbuk National University.

2.3. Histological techniques

For histological processing, liver tissues were fixed in phosphate buffer containing 10% formaldehyde and decalcified with EDTA. Fixed tissues were processed by routine methods to paraffin blocks. Specimens were sectioned at 4 μm and stained with H&E.

2.4. Western blot analysis

Homogenized liver tissues lysed by protein extraction solution (PRO-PREP, iNtRONBiotechnology, Korea) containing protease inhibitor cocktail (Calbiochem, Germany) and phosphatase inhibitor cocktail (Roche, Germany). Total proteins (30 μg) were separated by SDS-PAGE and transferred to a PVDF membrane (Millipore, Billerica, MA). The membrane was blocked with 5% skim milk overnight and then incubated with primary antibodies (diluted 1:1000) for 1 h at room temperature. The membranes were immunoblotted with the following primary antibodies: primary mouse monoclonal antibodies directed against JNK, phospho-JNK, (Cell Signaling Technology, Beverly, MA, USA), primary rabbit polyclonal antibody directed against Bcl-2, Bax (Santa Cruz Biotechnology, Dallas, Texas, USA), PRDX6-SO3 (Abcam, Cambridge, MA, USA) and primary sheep polyclonal antibody directed against PRDX6 (Abcam, Cambridge, MA, USA). After washing with Tris-buffered saline containing 0.05% Tween-20 (TBST), the membrane was incubated with horseradish peroxidase-conjugated secondary antibodies (diluted 1:3000) for 1 h at room temperature. Binding of antibodies to the PVDF membrane was detected with enhanced chemiluminescence solution (Amersham Bioscience, UK) and X-ray film (AGFA, Belgium).

2.5. Immunohistochemistry

All specimens were fixed in formalin and embedded in paraffin for examination. Sections (4 μm thickness) were stained with H&E and analyzed by immunohistochemistry using primary rabbit monoclonal antibodies directed against nitrotyrosine (1 : 100 dilution, Biolegend, Abcam, UK) and secondary horseradish peroxidase-conjugated anti-mouse and anti-rat antibodies.

2.6. Isolation of liver mitochondria and cytoplasm

For most of the experiments liver mitochondria were isolated from mice by differential centrifugation [23]. Livers from mice were excised, washed with 0.25 M sucrose, and homogenized in an H-medium (225 mM mannitol, 75 mM sucrose, 2 mM HEPES, 0.05% bovine serum albumin, plus protease and phosphatase inhibitors). The homogenate was centrifuged at $800 \times g$ for 10 min, the pellet was removed, and the centrifugation process was repeated. The resulting supernatant was centrifuged at $8500 \times g$ for 15 min. The supernatant (cytoplasmic fraction) was collected and saved at −80 °C for future analysis. The pellet which represents the mitochondria fraction was washed with H-medium and the centrifugation repeated. The mitochondria were

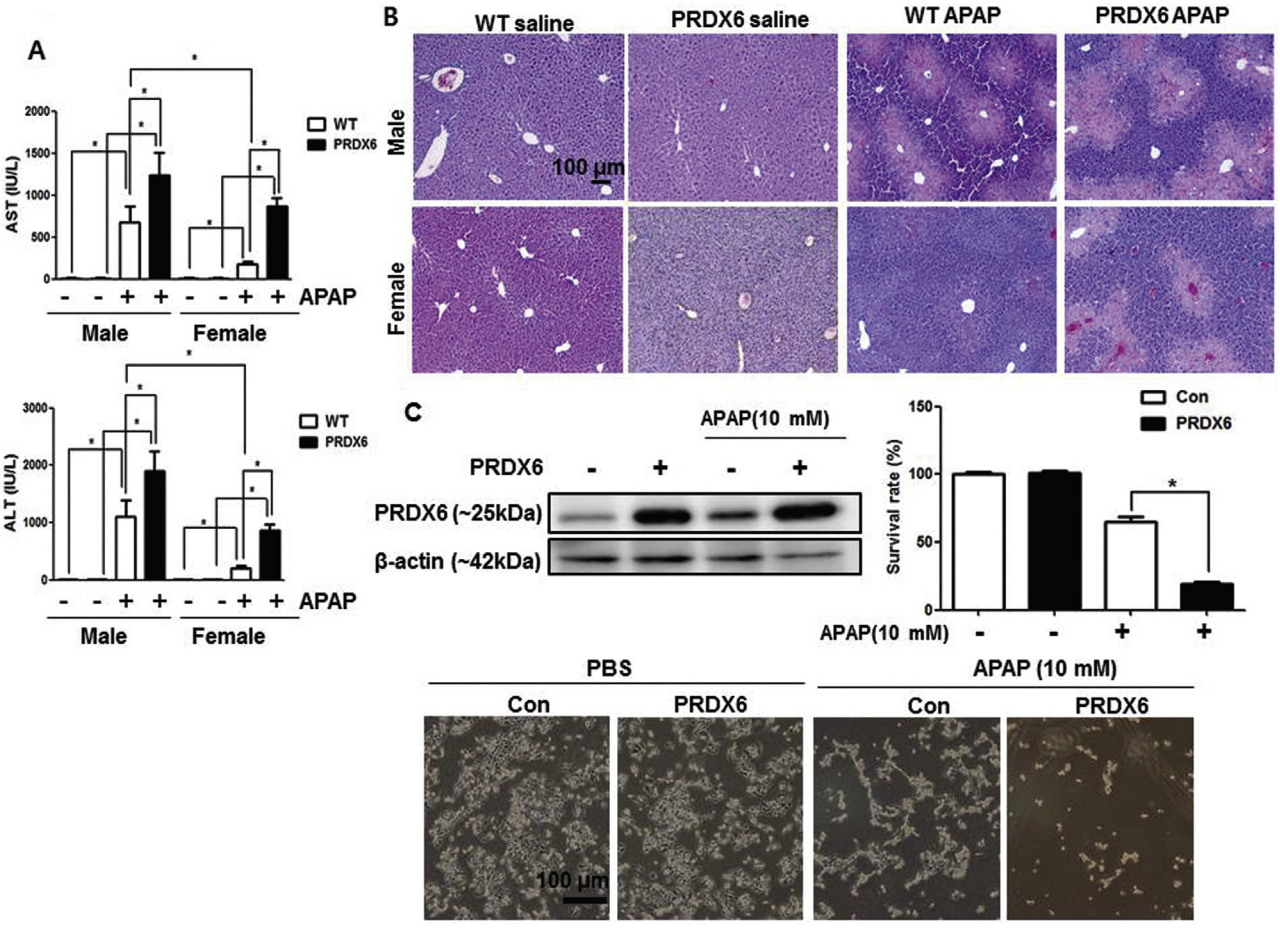

Fig. 1. PRDX6 overexpression enhances APAP-induced liver injury. (A) Serum AST and ALT levels in WT and PRDX6 mice with APAP administration (500 mg/kg) or without. n = 8 per group; means ± SEM, $^*P < 0.05$ (B) Liver sections of WT and PRDX6 mice with APAP administration (500 mg/kg) or without were stained with hematoxylin and eosin (H&E) (Scale bars, 100 μm). (C) Confirmation of PRDX6 overexpression in Huh7 cells then the survival rate and the picture of control or PRDX6 overexpressed Huh7 cells treated with APAP (10 mM) or without for 24 h. Values are expressed as the mean ± SEM of three different experiments conducted in triplicates. $^*P < 0.05$.

resuspended in H-medium before oxygen electrode and Western blot analysis.

2.7. Mitochondrial function assay

To investigate mitochondrial function in the liver of WT and PRDX6 mice, we use measurement of JC-1 mitochondrial membrane potential assay kit (Cayman Chemicals, Ann Arbor, MI).

2.8. Cell culture and cell survival assay

The human hepatic Huh7 cells were transfected with pcDNA3.1 plasmid vector (con), pCDNA 3.1 + PRDX6 (PRDX6). After O/N, cells were pretreated with JNK inhibitor, SP600125 (10 μg/ml) or PRDX6 inhibitor, MJ33 (30 μM) or N-acetylcysteine (NAC, positive control, 1 mM) or not for 3 h then treated with APAP (10 mM) for 24 h. For cell survival assay, MTT (3-(4,5-dimethylthiazol-2-yl)-2,5-diphenyltetrazolium bromide; Sigma, St Louis, MO, USA) diluted in DMEM medium, were added to each well and incubation was carried out for 90 min. Then, the supernatant was discarded and the crystal products were eluted with DMSO (200 μL/well; Sigma, St Louis, MO, USA). Colorimetric evaluation was performed with a spectrophotometer at 540 nm to detect cell growth.

2.9. Liver histopathology score

Histopathology scoring of liver sections, evaluating the degree of liver necrosis, was performed by a pathologist as previously described [24]. In brief, the grading was 0, no lesion present; 1/2, individual necrotic cells seen at the first cell layer adjacent to the central vein, and hyaline degeneration present; 1, necrotic cells extending two or three cell layers from the central veins; 2, necrotic cells extending three to six cell layers from the central veins, but limited in peripheral distribution; 3, the same as 2, but with necrosis extending from one central vein to another; 4, more severe than 3, with extensive centrilobular necrosis throughout the section.

2.10. Lysophosphatidylcholine measurement

To measure lysophosphatidylcholine in the liver of WT and PRDX6 mice and in hepatocytes, we use lysophosphatidylcholine assay kit (Biovision, Milpitas, CA, USA).

2.11. Calcium-independent phospholipase A_2 (iPLA2) activity assay

Calcium-independent phospholipase A_2 activities were measured according to the manufacturer's recommendations (Cayman Chemicals, Ann Arbor, MI). Cell pellets or liver tissues were suspended in 200 μl of 50 mM HEPES, pH 7.4, containing 1 mM EDTA, and sonicated at 10% power for 9 s with 9-s intervals for 10 times on ice. Supernatants were

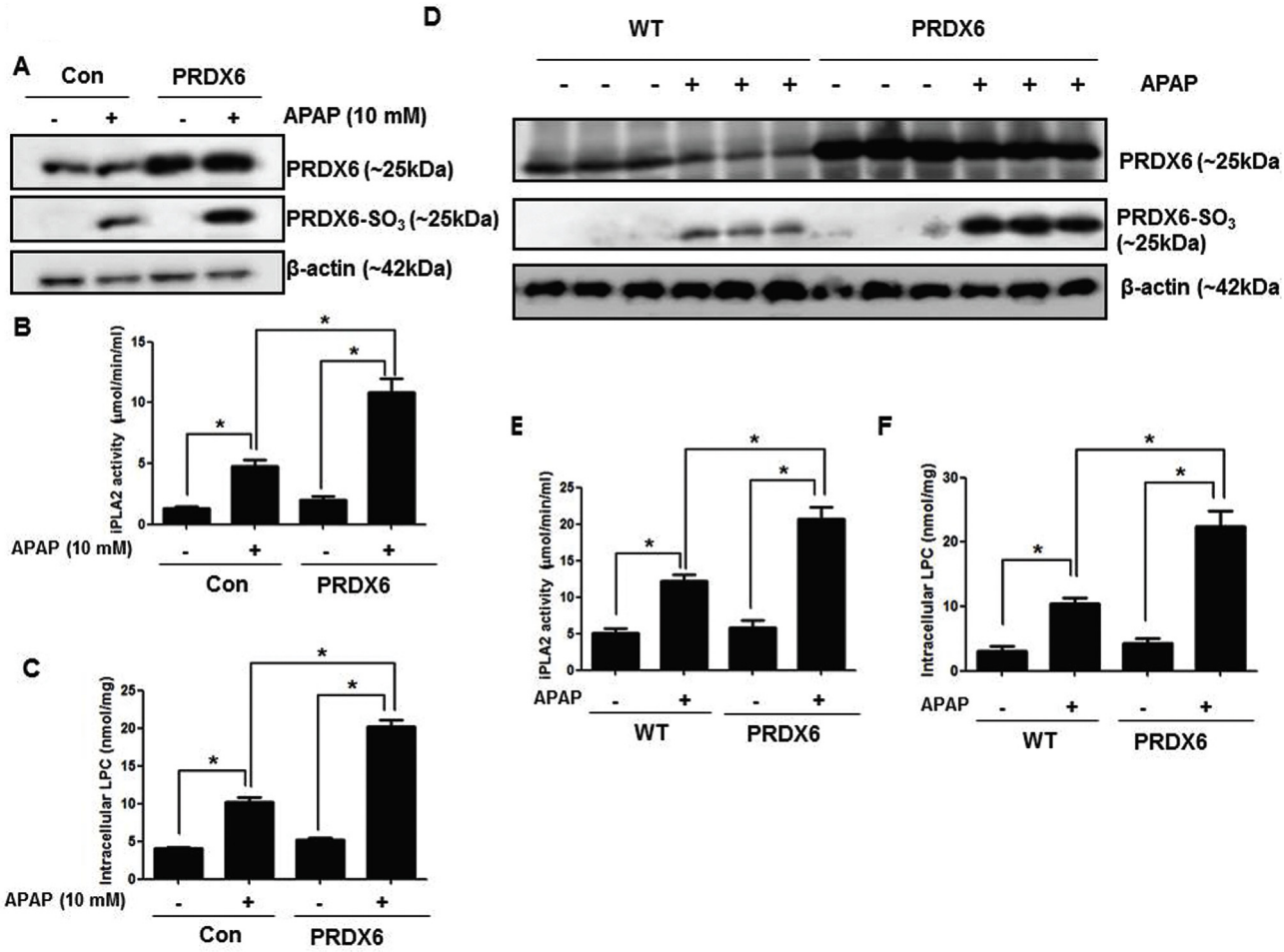

Fig. 2. APAP administration induced hyperoxidation of PRDX6, iPLA2 activity, and LPC levels in the liver of WT and PRDX6 mice. (A) Immunoblots of PRDX6 and PRDX6-SO_3 were determined in the control or PRDX6 overexpressed Huh7 cells by western blotting. (B) iPLA2 activity and (C) LPC level were measured in the control or PRDX6 overexpressed Huh7 cells. Values are expressed as the mean ± SEM of three different experiments conducted in triplicates. *$P < 0.05$. (D) Immunoblots of PRDX6 and PRDX6-SO_3 were determined in the liver of WT and PRDX6 mice with APAP administration or without. n = 3 per group. (E) iPLA2 activity and (F) LPC level were measured in the liver of WT and PRDX6 mice with APAP administration or without. . n = 8 per group; means ± SEM, *$P < 0.05$.

obtained by centrifugation at 10,000×*g* for 15 min at 4 ˚C. Supernatants containing 50 μg of protein in a total volume of 45 μl were added to microplate wells containing 5 μl of pf assay buffer with (iPLA2 activity) or without 10 μM BEL (total PLA2 activity). The reaction was initiated by addition of 200 μl of arachidonoyl thiophosphatidylcholine and was incubated at room temperature for 60 min. The reaction was terminated by addition of 10 μl of 25 mM 5,5′-dithio-bis(2-nitrobenzoic acid), and the absorbance was measured at 405 nm in an Emax precision microplate reader (Molecular devices). The iPLA2 activity was calculated according to the manufacturer's instructions.

2.12. Statistical analysis

The experiments were conducted either in triplicate, and all experiments were repeated at least three times with similar results. The data were analyzed using the GraphPad Prism 4 version 4.03 software (GraphPad Software, La Jolla, CA). Data are presented as mean ± SEM. The differences in all data were assessed by one-way analysis of variance. When the P value in the analysis of variance test indicated statistical significance, the differences were assessed by the Tukey's test.

3. Results

3.1. PRDX6 overexpression demonstrates high sensitivity to APAP-induced acute liver injury but did not prevent APAP-induced oxidative stress

To examine the effects of PRDX6 in drug-induced liver injury, both male and female WT or PRDX6 mice were administered an overdose of APAP by i.p. injection (500 mg/kg). In WT mice, APAP-induced AST and ALT levels were significantly reduced in female mice compared to male mice (Fig. 1A). However, APAP-induced AST and ALT levels were markedly increased in both male and female PRDX6 mice compared to the respective WT mice (Fig. 1A). Histological analysis revealed massive liver damage in APAP-injected male WT mice and this damage was extremely severe in the liver of PRDX6 mice (Fig. 1B). Comparable with the ALT and AST levels, female WT mice demonstrated mild hepatic injury in APAP-injected liver compared to male WT mice; whereas, both female and male PRDX6 mice showed severe hepatic injury in the APAP-injected liver compared to WT mice (Fig. 1B). APAP induces mitochondrial GSH depletion at an early time point in the liver; thus, we investigated oxidative stress in the APAP-induced liver of WT and PRDX6 mice. Our data indicated that both WT and PRDX6 mice demonstrated significant mitochondrial GSH depletion in the liver 6 h after the APAP injection; however, no difference was observed between WT and PRDX6 mice following APAP administration (Supplementary Fig. 1A). No differences were observed in the APAP-induced liver

mitochondrial hydrogen peroxide levels between APAP-injected WT and PRDX6 mice (Supplementary Fig. 1A). The APAP-induced CYP2E1 expression demonstrated no difference between WT and PRDX6 mice (Supplementary Fig. 1B). As PRDX6 overexpression promotes APAP-induced liver injury, we examined the effect of PRDX6 overexpression on APAP-induced cell damage in human hepatic Huh7 cells. We transfected Huh7 cells with the PRDX6 expressing vector and confirmed the expression of PRDX6 by western blotting (Fig. 1C). In APAP-treated Huh7 cells, the survival rate decreased in PRDX6 overexpressing cells compared to the control cells (Fig. 1C); however, similar to the in vivo results, APAP-induced CYP2E1 expression did not significantly differ between the PRDX6 overexpressing cells and control cells (Supplementary Fig. 1C). Additionally, no significant differences were observed between the mitochondrial intracellular hydrogen peroxide and GSH depletion levels in PRDX6 overexpressing cells and control cells (Supplementary Fig. 1D).

3.2. APAP enhances iPLA2 activity and LPC levels through PRDX6 hyperoxidation

Recently, a study has reported that the hyperoxidative condition results in the formation of PRDX6-sulfonic acid (PRDX6-SO3), a hyperoxidative form of PRDX6. PRDX6-SO3 induces hepatocyte apoptosis through the upregulation of the iPLA2 activity of PRDX6 [25]. In addition, LPC, generated from phosphatidylcholine (PC) by iPLA2, induces hepatocyte apoptosis [26]. We observed that exogenous LPC induced cell death and LPC and APAP co-treatment induced marked cell death in mouse primary hepatocytes (Supplementary Fig. 2). Thus, APAP administration could induce PRDX6 hyperoxidation and hyperoxidized PRDX6 may result in liver injury by increasing LPC levels via elevated iPLA2 activity. To confirm these effects, we transfected Huh7 cells with control and PRDX6 expressing vectors, followed by APAP treatment. Hyperoxidation of PRDX6 was monitored by employing specific antibodies recognizing PRDX6-SO_3. In APAP-treated Huh7 cells, PRDX6 was hyperoxidized following APAP treatment and PRDX6-SO_3 was further increased in PRDX6 overexpressing Huh7 cells compared to control Huh7 cells treated with APAP (Fig. 2A). These results suggested that overexpressed PRDX6 was converted to the hyperoxidized form by APAP administration. The iPLA2 activity and LPC were also increased by APAP; these activities were further increased in PRDX6 overexpressing Huh7 cells compared to control Huh7 cells treated with APAP (Fig. 2B and C). Like Huh7 cells, following APAP administration, PRDX6 was hyperoxidized in the liver of WT mice and PRDX6-SO_3 was further increased in PRDX6 mice compared to WT mice administered APAP (Fig. 2D). Additionally, iPLA2 activity and LPC were increased in the liver of WT mice following APAP administration; these levels were further increased in the liver of APAP-injected PRDX6 mice compared to APAP-injected WT mice (Fig. 2E and F).

3.3. The iPLA2 activity of PRDX6 inhibitor, MJ33, attenuates APAP-induced liver injury

As APAP-induced PRDX6 hyperoxidation increased iPLA2 activity and LPC levels and PRDX6 overexpression promoted APAP-induced liver injury, we investigated whether the iPLA2 activity of PRDX6 inhibitor, MJ33, affected APAP-induced liver injury. Firstly, we evaluated the adverse effects of MJ33 in the mouse primary hepatocytes and observed that MJ33 demonstrated no cytotoxic effects (Supplementary Fig. 3A). The histological analysis revealed that the APAP-induced extensive liver damage in both WT and PRDX6 mice was attenuated following the administration of MJ33 (Fig. 3A and B). Additionally, we observed that the MJ33 injection decreased APAP-induced ALT and AST levels in the serum of both WT and PRDX6 mice (Fig. 3C). Moreover, MJ33 attenuated APAP-induced cell death in mouse primary hepatocytes like NAC (positive control) (Supplementary Fig. 3B). To investigate whether MJ33 affects APAP-induced oxidative stress, we pretreated APAP-treated mouse primary hepatocytes with MJ33 or NAC and then measured GSH and hydrogen peroxide levels. We observed that the PRDX6 inhibitor, MJ33, did not affect APAP-induced GSH depletion unlike NAC; however, MJ33 inhibited APAP-induced hydrogen peroxide production s NAC. (Supplementary Figs. 3C and D). Following APAP administration, iPLA2 activity and LPC levels were further increased in the liver of PRDX6 mice compared to WT mice; these increased levels were restored following MJ33 administration in APAP-injected PRDX6 mice to the same level as APAP-injected WT mice (Fig. 3D and E). In addition, APAP-induced PRDX6-SO3 was decreased by MJ33 (Fig. 3F). These results suggested that MJ33 inhibits the iPLA2 activity of PRDX6 by abrogating PRDX6 hyperoxidation induced by APAP. Next, we examined whether the PRDX6 inhibitor, MJ33, affected APAP-induced iPLA2 activity and LPC levels in primary mouse hepatocytes from WT and PRDX6 mice. In both PRDX6 overexpressing cells and control cells, MJ33 restored the decreased cell survival rates induced by APAP treatment (Fig. 4A). In addition, following APAP treatment, the increased iPLA2 activity and LPC levels were restored by MJ33 in APAP-treated PRDX6-overexpressing and control cells (Fig. 4B and C).

3.4. Overexpression of PRDX6 enhances mitochondrial dysfunction by APAP by increasing JNK activation

Mitochondria are a major organelle in APAP-induced liver injury and its dysfunctions are closely associated with hepatic necrosis. Compared to saline-injected WT and PRDX6 mice, the ratio of J-aggregates (heathy) to J-monomers (unhealthy) in the liver was decreased in the liver of APAP-injected WT and PRDX6 mice. However, the ratio of J-aggregates to J-monomers in the liver of APAP-injected PRDX6 mice was markedly decreased compared to APAP-injected WT mice (Fig. 5A). JNK activation and subsequent translocation into the mitochondria are critical factors of mitochondrial dysfunction in the APAP-induced liver injury model. Furthermore, we observed that PRDX6 mice demonstrated enhanced susceptibility to APAP-induced liver injury compared to WT mice. Hence, we investigated JNK activation in the liver of WT and PRDX6 mice. Compared to APAP-injected WT mice, we observed that JNK was considerably activated in the APAP-injected PRDX6 mice (Fig. 5B). Next, we investigated the mitochondrial translocation of phosphor-JNK in the liver of APAP-injected WT and PRDX6 mice. Compared to APAP-injected WT mice, phosphor-JNK was increased in the mitochondrial fraction of APAP-injected PRDX6 liver (Fig. 5C). Bcl-2, known as an anti-apoptotic protein, demonstrated no difference between the APAP-injected WT mice with APAP-injected PRDX6 mice; however, Bax, a known apoptotic protein, was increased in the mitochondrial fraction of APAP-injected PRDX6 liver compared to APAP-injected WT mice (Fig. 5C). In APAP-treated Huh7 cells, phosphorylated JNK and Bax were increased in the mitochondrial fraction of PRDX6 overexpressing cells compared to control cells, as seen in the in vivo data (Supplementary Fig. 4A). Next, we investigated whether MJ33 affected APAP-induced JNK activation as PRDX6 overexpression induced JNK activation in the liver and hepatocytes. As observed in iPLA2 activity and LPC measurement data, following APAP administration, JNK activation was further increased in PRDX6 mice compared to WT mice. However, MJ33 diminished JNK activation in the liver of both WT and PRDX6 mice (Fig. 5E). Additionally, the increased translocation of phosphor-JNK into the mitochondria and mitochondrial fraction of Bax following APAP administration were decreased by MJ33 in the liver of both WT and PRDX6 mice (Fig. 5F). In APAP-treated Huh7 cells, APAP-induced JNK activation was markedly activated in PRDX6 overexpressing cells; the levels were restored by MJ33 in APAP-treated PRDX6 overexpressing cells and control cells (Supplementary Fig. 4B). Moreover, MJ33 also inhibited JNK activation and apoptotic signals, including Bax and cleaved caspase 3, induced by APAP in mouse primary hepatocytes (Supplementary Fig. 4C).

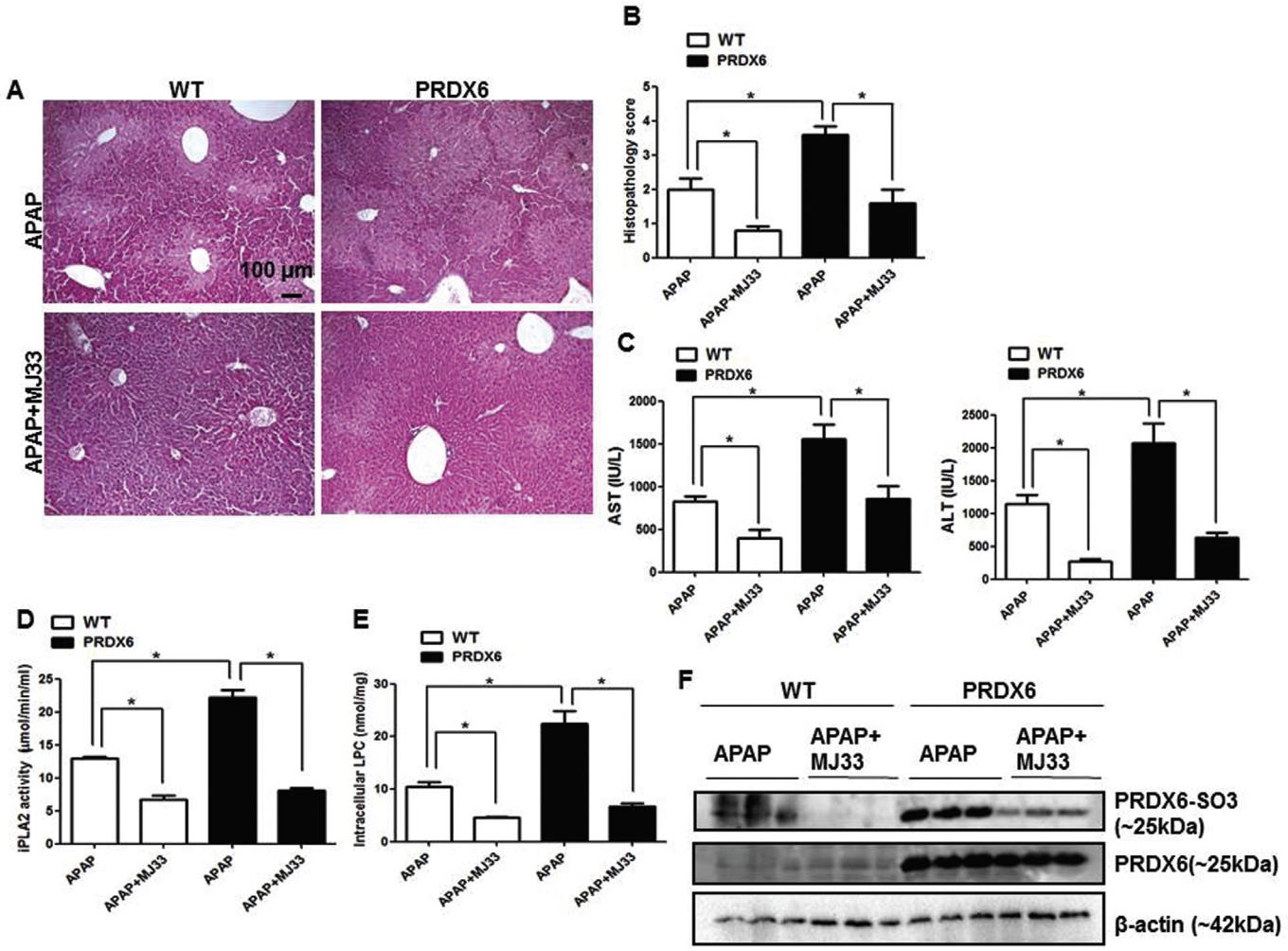

Fig. 3. PRDX6 inhibitor, MJ33 attenuates APAP-induced liver injury both WT and PRDX6 mice. (A) Liver sections of WT and PRDX6 mice with PRDX6 inhibitor, MJ33 pre-injection (2.5 nmol/g) or not then APAP (500 mg/kg) administration were stained with hematoxylin and eosin (H&E) (Scale bars, 100 μm), and (B) histopathology score. (C) Serum AST and ALT levels in WT and PRDX6 mice pre-injected MJ33 (2.5 nmol/g) or not then administration with APAP (500 mg/kg) or without. n = 8 per group; means ± SEM, $^*P < 0.05$. (D) iPLA2 activity and (E) LPC level were measured in the liver of WT and PRDX6 mice MJ33 pre-injection (2.5 nmol/g) or not then APAP (500 mg/kg) administration. n = 8 per group; means ± SEM, $^*P < 0.05$. (F) Immunoblots of PRDX6 and PRDX6-SO_3 were determined in the liver of WT and PRDX6 mice pre-injected pre-injected MJ33 (2.5 nmol/g) or not then administration with APAP (500 mg/kg). n = 3 per group.

3.5. JNK inhibitor abrogates APAP-induced liver injury both WT and PRDX6 mice

We observed that PRDX6 mice showed enhanced JNK activation induced by APAP. Hence, we investigated whether the JNK inhibitor, SP600125, affected hyperoxidation of PRDX6, iPLA2 activity, and LPC levels induced by APAP and whether it attenuated APAP-induced liver injury in WT and PRDX6 mice. In both WT and PRDX6 mice, the histological evaluation revealed the APAP-induced extensive liver damage was diminished following the administration of the JNK inhibitor (Fig. 6A and B). Moreover, we observed that the JNK inhibitor decreased APAP-induced ALT and AST levels in the serum of both WT and PRDX6 mice; however, the degree of reduction was greater in the PRDX6 mice (Fig. 6C). In addition, phosphor-JNK and Bax levels were greatly increased in the liver mitochondrial fraction of the APAP-injected PRDX6 mice compared to APAP-injected WT mice (Fig. 6D). In APAP-treated Huh7 cells, treatment with the JNK inhibitor recovered the survival rate in both control cells and PRDX6 overexpressing cells (Fig. 6E). These results suggested that the JNK inhibitor abrogated APAP-induced liver injury in both WT and PRDX6 mice. However, the JNK inhibitor did not affect APAP-induced hyperoxidation of PRDX6 (Supplementary Fig. 5A), iPLA2 activity, and LPC levels in the liver of WT and PRDX6 mice (Supplementary Fig. 5B and C). These results suggested that PRDX6 was hyperoxidized by APAP and hyperoxidized PRDX6 increased iPLA2 activity and LPC levels. Finally, this cascade enhanced JNK activation; the JNK inhibitor only abrogated JNK activation, a final step in APAP-induced hepatotoxicity.

4. Discussion

This study revealed the unexpected role of PRDX6 in APAP-induced liver injury. Like other PRDXs members, PRDX6 is known to play a role in antioxidant defense, but our data demonstrated that overexpression of PRDX6 failed to scavenge the ROS induced by APAP, further exacerbating the APAP-induced liver injury. Previously, a study reported that the overexpression of PRDX6 does not prevent the oxidative stress induced by chronic ethanol consumption [12]. PRDX6 is a member of the PRDX family, which are non-seleno peroxidases. However, unlike the other PRDXs, PRDX6 has an important distinguishing characteristic; it is a bifunctional enzyme with glutathione peroxidase and PLA_2 activities [13]. The role of PRDX6 in APAP-induced acute liver injury remains completely unknown and was hence investigated in this study.

APAP-induced liver injury is initially mediated by the formation of NAPQI, a reactive metabolite generated during the metabolism of APAP

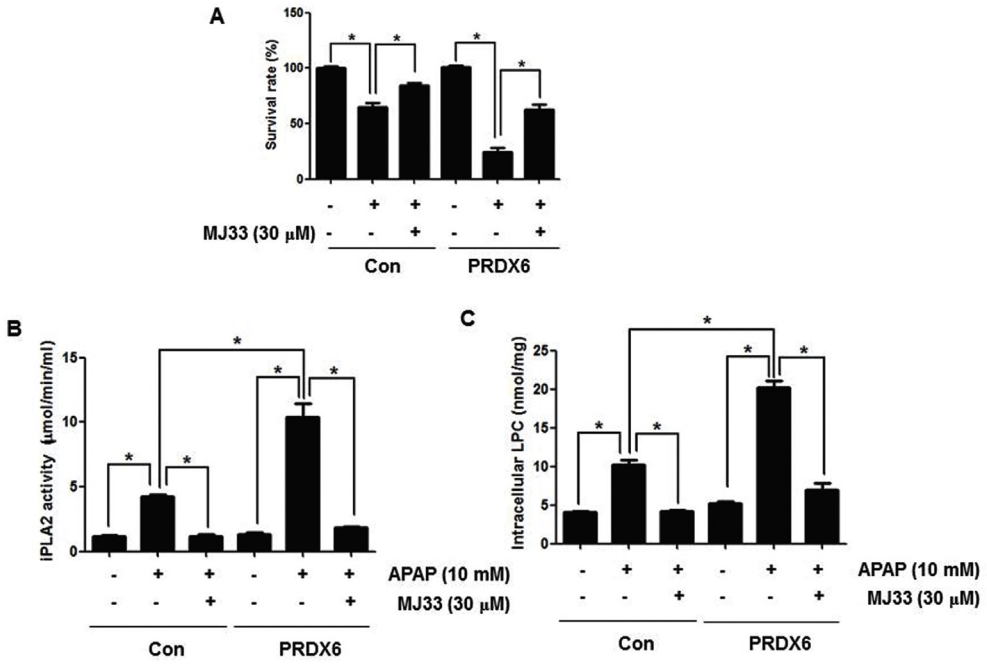

Fig. 4. PRDX6 inhibitor, MJ33 abrogates APAP-induced hepatotoxity in Huh7 human hepatocytes. (A) The survival rate of the control or PRDX6 overexpressed Huh7 cells pre–treated with PRDX6 inhibitor, MJ33 (30 μM) or not then treated with APAP (10 mM) or without for 24 h. Values are expressed as the mean ± SEM of three different experiments conducted in triplicates. $^{*}P < 0.05$. (B) iPLA2 activity and (C) LPC level were measured in in the control or PRDX6 overexpressed Huh7 cells pretreated with MJ33 or without then APAP administration. Values are expressed as the mean ± SEM of three different experiments conducted in triplicates. $^{*}P < 0.05$.

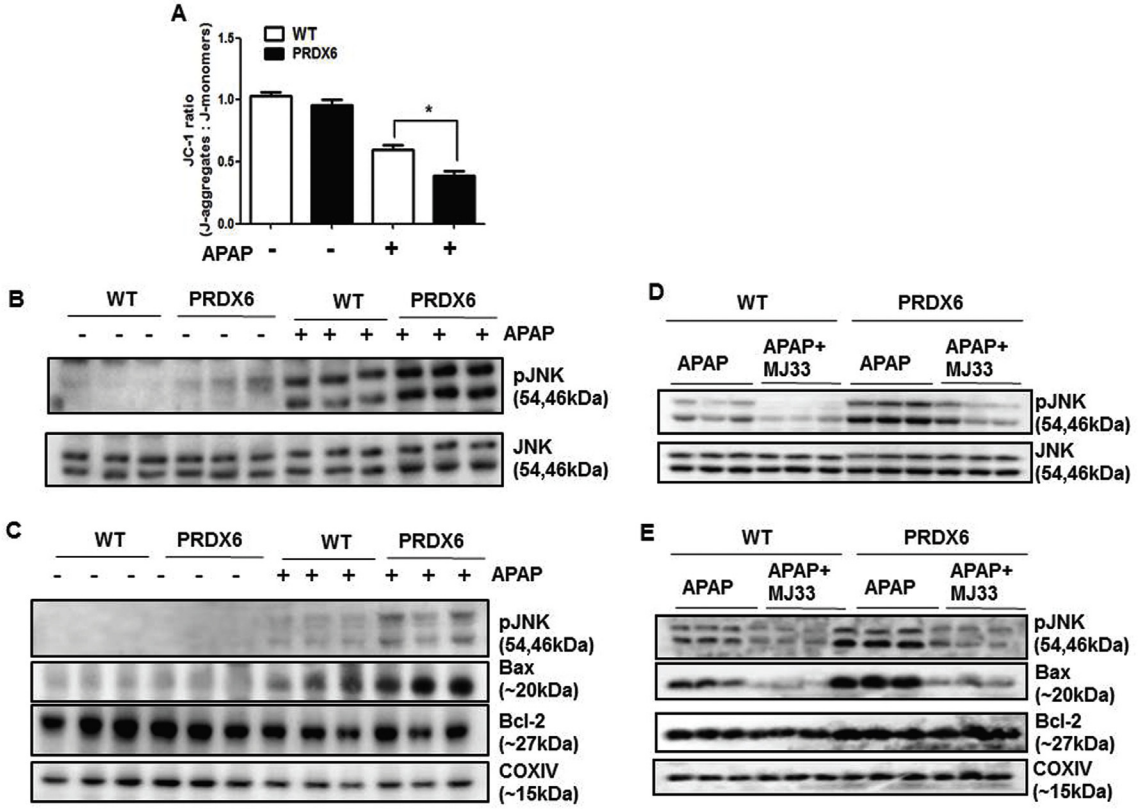

Fig. 5. PRDX6 overexpression promotes mitochondrial dysfunction through enhancing APAP-induced JNK phosphorylation in the liver of mice. (A) Mitochondrial integrity in the liver of WT mice and PRDX6 mice with APAP administration (500 mg/kg) or without n = 8 per group; means ± SEM, $^{*}P < 0.05$ (B) Immunoblots of pJNK and JNK were determined in the total protein extracts of mice liver tissues and (C) immunoblots of pJNK, Bax, and Bcl-2 were determined in the mitochondrial fraction of mice liver tissues by western blotting. COXIV as a mitochondrial biomarker. n = 3 per group (D) Immunoblots of pJNK and JNK were determined in the liver of WT and PRDX6 mice pre-injected pre-injected MJ33 (2.5 nmol/g) or not then administration with APAP (500 mg/kg) and (E) immunoblots of pJNK, Bax, and Bcl-2 were determined in the mitochondrial fraction of mice liver tissues by western blotting. COXIV as a mitochondrial biomarker. n = 3 per group.

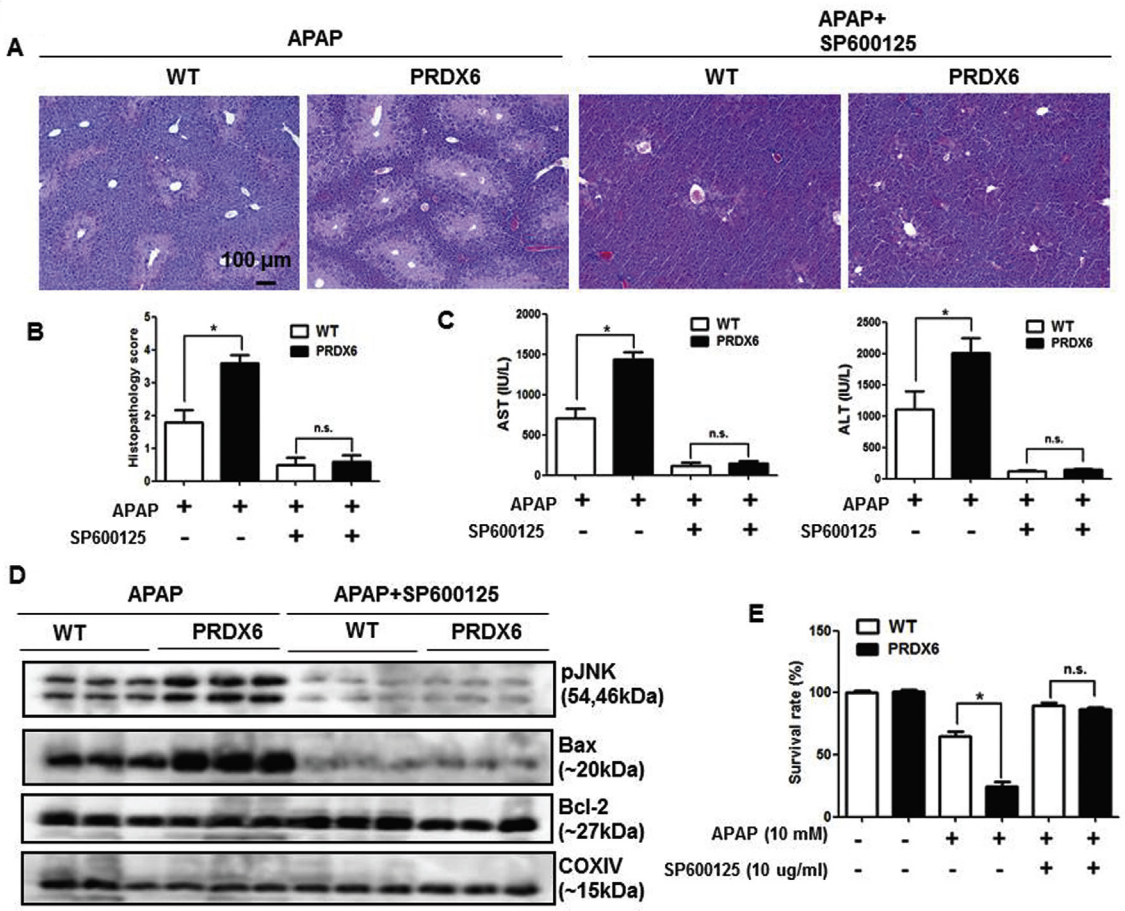

Fig. 6. Enhanced effects by PRDX6 overexpression in the APAP-induced liver injury was abrogated by JNK inhibitor, SP600125 (A) Liver sections of WT and PRDX6 mice with JNK inhibitor, SP600125 pre-injection (10 mg/kg) or not then APAP administration (500 mg/kg) or not were stained with hematoxylin and eosin (H&E) (Scale bars, 100 μm), and (B) histopathology score. (C) Serum AST and ALT levels in WT and PRDX6 mice pre-injected SP600125 (10 mg/kg) or not then administration with APAP (500 mg/kg) or without. n = 8 per group; means ± SEM, $^*P < 0.05$ (D) Immunoblots of pJNK, Bax, and Bcl-2 were determined in the mitochondrial fraction of mice liver tissues by western blotting. COXIV as a mitochondrial biomarker. n = 3 per group (E) The survival rate of the control or PRDX6 overexpressed Huh7 cells pre–treated with JNK inhibitor, SP600125 (10 μg/ml) or not then treated with APAP (10 mM) or without for 24 h. Values are expressed as the mean ± SEM of three different experiments conducted in triplicates. $^*P < 0.05$.

by cytochrome P450 (primarily the CYP2EI isoform) [3]. GSH undergoes conversion and is then excreted via the bile after glucuronidation [2]. At hepatotoxic doses of APAP, the antioxidant GSH, which can convert NAPQI into a harmless reduced form, is severely depleted in the cytoplasm and mitochondria. Han et al. have suggested the 'two-hit model' of APAP hepatotoxicity, which involves a complex feed-forward loop that involves two injuries to the mitochondria [27]. The first mitochondrial injury involves mitochondrial GSH depletion and covalent binding by NAPQI. NAPQI can bind to thiols in the respiratory complexes [28] and deplete mitochondrial GSH needed by GSH peroxidase, detoxifying hydrogen peroxide [29]. These factors are likely to be important in enhancing mitochondrial ROS generation following APAP treatment. In our data, PRDX6 mice showed more severe liver damage following APAP administration compared to WT mice; however, following APAP administration, CYP2E1 expression and GSH depletion in the liver of PRDX6 mice did not differ from that of WT mice. Moreover, APAP-induced mitochondrial GSH depletion and hydrogen peroxide levels did not significantly differ between the livers of PRDX6 mice and WT mice. These results suggested that PRDX6, as an antioxidant enzyme, was not associated with the processing of APAP metabolism and preventing of APAP-induced oxidative stress in the mitochondria. Thus, we questioned the rationale behind the enhanced susceptibility to APAP-induced liver injury observed in PRDX6 mice.

PRDX6 demonstrates bifunctional ability as glutathione peroxidase and mediates PLA_2 activity [13]. Furthermore, these activities were regulated by the environment, including oxidation and pH specificity [30]. Kim et al. have reported that a high concentration of hydrogen peroxidase induces hyperoxidation of PRDX6 and leads to cell death via increasing iPLA2 activity [25]. Moreover, LPC, a lipid metabolite generated by iPLA2, induces hepatocyte cell death through GSK-3/JNK and is associated with mitochondrial dysfunction via PUMA/Bax [26]. Thus, we hypothesized that PRDX6 was hyperoxidized by APAP and the hyperoxidized PRDX6 increased iPLA2 activity. Then, the increased iPLA2 activity exacerbated APAP-induced hepatotoxicity by elevating the LPC level. In the present study, we observed that, following the administration of the APAP injection, hyperoxidation of PRDX6, iPLA2 activity, and LPC levels were increased in the livers of both the WT and PRDX6 mice; however, these levels were markedly increased in the liver of APAP-injected PRDX6 mice compared to WT mice. In hepatocytes, PRDX6 overexpression further increased the iPLA2 activity under high concentrations of hydrogen peroxide [25]. MJ33 is known to competitively inhibit the PLA_2 activity of PRDX6 [13]. In our data, MJ33 ameliorated APAP-induced liver injury in PRDX6 mice and APAP-induced toxicity in hepatocytes by decreasing PRDX6 hyperoxidation, iPLA2 activity, and LPC levels. These results suggested that PRDX6 was converted to the hyperoxidized form by the APAP-induced high concentration of hydrogen peroxides, and hyperoxidized PRDX6 induced cellular toxicity in the liver by elevating iPLA2 activity and LPC levels.

ROS inhibits the pro-survival transcription factor NF-κB and subsequently triggers the autophosphorylation and activation of JNK [20]. The activated JNK leads to mitochondrial membrane permeabilization and dysfunction, which is the second injury to the mitochondria [7]. In our data, compared to WT mice, PRDX6 mice demonstrated enhanced JNK activation in the liver after APAP administration. Compared to control cells, PRDX6 overexpression leads to marked cell death and JNK activation following APAP treatment in human hepatic Huh7 cells. Here, we used human hepatic Huh7 cells to mimic the human liver. We planned to attempt an in vitro experiment using human primary hepatic cells; however, owing to the cost of the experiment and difficulty in handling, this plan was abandoned. Kuo et al. have reported this limited availability of human primary human hepatic cells in an APAP toxicity study [31]. Furthermore, Lin et al. have documented that Huh-7 and HCC-T cells are potential cells to study drug metabolism among the five human hepatoma cell lines (HepG2, Hep3B, HCC-T, HCC-M, and Huh7) [32]. Thus, we selected Huh7 cells to evaluate APAP toxicity study in the human liver. Activated JNK translocates to the mitochondria and binds to Sab, a scaffold protein on the outer membrane of mitochondria that contains a kinase interaction motif [16], phosphorylating Sab. This results in increased Bax levels, inducing mitochondrial permeability transition in damaged mitochondria [20]. In the present study, compared to WT mice, PRDX6 mice demonstrated increased phosphor-JNK and Bax levels in the liver mitochondria after APAP administration. In addition, compared to the control, in Huh7 cells, PRDX6 overexpression also further increased APAP-induced phosphor-JNK and Bax levels in the mitochondria.

Recently, Du et al. have reported that female mice demonstrated lower susceptibility in APAP-induced liver injury [21]. They observed that there is no gender difference in the metabolic activation of APAP, as well as GSH depletion, but female mice showed lower JNK activation compared to male mice after APAP administration. Moreover, Mohar et al. have reported that female mice showed lower susceptibility in APAP-induced liver injury and PRDX6 was preferentially adducted by APAP in male mice, but rarely adducted in female mice [22]. In our data, female mice also demonstrated lower susceptibility in APAP-induced liver injury compared to male mice; however, PRDX6 mice demonstrated further exacerbation of APAP-induced liver injury in both male and female mice. In addition, we observed that PRDX6 overexpression further increased JNK activation in the mouse liver tissue or Huh7 human hepatocytes after APAP administration. Thus, we hypothesized that PRDX6 and its adduction were closely associated with JNK activation in APAP-induced liver injury and we questioned how PRDX6 enhanced JNK activation. Previously, we have demonstrated that PRDX6 overexpression exacerbates collagen antibody-induced arthritis (CAIA) by enhancing JNK activation and the JNK inhibitor or MJ33 attenuates CAIA by inhibiting JNK activation in PRDX6 mice [15]. Moreover, increasing iPLA2 activity and elevating LPC induces hepatocyte cell death through JNK activation [26]. Thus, JNK activation by PRDX6 may be abrogated by MJ33. In our data, MJ33 decreased APAP-induced JNK activation in the liver and hepatocytes. These results suggested that hyperoxidized PRDX6 induces JNK activation by increasing iPLA2 activity and LPC level.

Next, we examined whether JNK inhibition affected the APAP-induced PRDX6 hyperoxidation-iPLA2-LPC cascade. Although SP600125, the JNK inhibitor, abolished APAP-induced liver injury in both WT and PRDX6 mice and restored cell viability in control and PRDX6-overexpressed Huh7 cells after APAP treatment, the restoration rate was markedly increased in PRDX6 mice and PRDX6-overexpressed Huh7 cells compared to the respective controls. However, the JNK inhibitor did not affect APAP-induced hyperoxidation of PRDX6, iPLA2 activity, and LPC levels in the liver of WT and PRDX6 mice. Notably, SP600125 perfectly attenuated APAP-induced liver injury in the liver of WT and PRDX6 mice. These results suggested that the JNK inhibitor abrogates APAP-induced liver injury in both WT and PRDX6 mice and, by enhancing JNK activation, exacerbates APAP-induced liver injury by PRDX6 overexpression, probably by only this pathway.

5. Conclusion

In summary, our results indicate that PRDX6 overexpression exacerbates APAP-induced liver injury. PRDX6 overexpression does not affect the metabolic activation of APAP, as well as GSH depletion, but promotes mitochondrial dysfunction by enhancing APAP-induced JNK phosphorylation in the liver of mice and hepatocytes. MJ33 inhibits the enhanced effects of PRDX6 overexpression in the APAP-induced liver injury. Additionally, the JNK inhibitor also abolished APAP-induced injury but failed to affect the PRDX6 hyperoxidation-iPLA2 activity-LPC cascade. These results suggest that, under the APAP-induced elevated hydrogen peroxide conditions, hyperoxidized PRDX6 enhances cellular toxicity in the liver through JNK activation by enhancing iPLA2 activity and LPC levels; this mechanism is a one-way cascade.

Funding

This research was supported by the National Research Foundation of Korea [NRF] Grant funded by the Korea government (MSIP) (No. MRC2017R1A5A2015541).

Declaration of competing interest

The authors declare that they have no competing interest.

Appendix A. Supplementary data

Supplementary data to this article can be found online at https://doi.org/10.1016/j.redox.2020.101496.

References

[1] A.M. Larson, et al., Acetaminophen-induced acute liver failure: results of a United States multicenter, prospective study, Hepatology 42 (6) (2005) 1364–1372.
[2] F.S. Larsen, J. Wendon, Understanding paracetamol-induced liver failure, Intensive Care Med. 40 (6) (2014) 888–890.
[3] D.C. Dahlin, et al., N-acetyl-p-benzoquinone imine: a cytochrome P-450-mediated oxidation product of acetaminophen, Proc. Natl. Acad. Sci. U. S. A. 81 (5) (1984) 1327–1331.
[4] S.D. Cohen, et al., Selective protein covalent binding and target organ toxicity, Toxicol. Appl. Pharmacol. 143 (1) (1997) 1–12.
[5] L.L. Meyers, et al., Acetaminophen-induced inhibition of hepatic mitochondrial respiration in mice, Toxicol. Appl. Pharmacol. 93 (3) (1988) 378–387.
[6] H. Jaeschke, Glutathione disulfide formation and oxidant stress during acetaminophen-induced hepatotoxicity in mice in vivo: the protective effect of allopurinol, J. Pharmacol. Exp. Therapeut. 255 (3) (1990) 935–941.
[7] J.W. Chambers, P.V. LoGrasso, Mitochondrial c-Jun N-terminal kinase (JNK) signaling initiates physiological changes resulting in amplification of reactive oxygen species generation, J. Biol. Chem. 286 (18) (2011) 16052–16062.
[8] S.G. Rhee, et al., Peroxiredoxin, a novel family of peroxidases, IUBMB Life 52 (1–2) (2001) 35–41.
[9] C.S. Yang, et al., Roles of peroxiredoxin II in the regulation of proinflammatory responses to LPS and protection against endotoxin-induced lethal shock, J. Exp. Med. 204 (3) (2007) 583–594.
[10] J.Y. Huh, et al., Peroxiredoxin 3 is a key molecule regulating adipocyte oxidative stress, mitochondrial biogenesis, and adipokine expression, Antioxidants Redox Signal. 16 (3) (2012) 229–243.
[11] A. Nabeshima, et al., Peroxiredoxin 4 protects against nonalcoholic steatohepatitis and type 2 diabetes in a nongenetic mouse model, Antioxidants Redox Signal. 19 (17) (2013) 1983–1998.
[12] J.R. Roede, et al., Overexpression of peroxiredoxin 6 does not prevent ethanol-mediated oxidative stress and may play a role in hepatic lipid accumulation, J. Pharmacol. Exp. Therapeut. 330 (1) (2009) 79–88.
[13] A.B. Fisher, Peroxiredoxin 6: a bifunctional enzyme with glutathione peroxidase and phospholipase A(2) activities, Antioxidants Redox Signal. 15 (3) (2011) 831–844.
[14] J.W. Chen, et al., 1-Cys peroxiredoxin, a bifunctional enzyme with glutathione peroxidase and phospholipase A2 activities, J. Biol. Chem. 275 (37) (2000) 28421–28427.
[15] D.H. Kim, et al., Exacerbation of collagen antibody-induced arthritis in transgenic mice overexpressing peroxiredoxin 6, Arthritis Rheum. 67 (11) (2015) 3058–3069.
[16] C. Wiltshire, et al., A new c-Jun N-terminal kinase (JNK)-interacting protein, Sab (SH3BP5), associates with mitochondria, Biochem. J. 367 (Pt 3) (2002) 577–585.

[17] S. Win, et al., c-Jun N-terminal kinase (JNK)-dependent acute liver injury from acetaminophen or tumor necrosis factor (TNF) requires mitochondrial Sab protein expression in mice, J. Biol. Chem. 286 (40) (2011) 35071–35078.
[18] S. Win, et al., c-Jun N-terminal kinase mediates mouse liver injury through a novel Sab (SH3BP5)-dependent pathway leading to inactivation of intramitochondrial Src, Hepatology 63 (6) (2016) 1987–2003.
[19] B.K. Gunawan, et al., c-Jun N-terminal kinase plays a major role in murine acetaminophen hepatotoxicity, Gastroenterology 131 (1) (2006) 165–178.
[20] N. Hanawa, et al., Role of JNK translocation to mitochondria leading to inhibition of mitochondria bioenergetics in acetaminophen-induced liver injury, J. Biol. Chem. 283 (20) (2008) 13565–13577.
[21] K. Du, et al., Lower susceptibility of female mice to acetaminophen hepatotoxicity: role of mitochondrial glutathione, oxidant stress and c-jun N-terminal kinase, Toxicol. Appl. Pharmacol. 281 (1) (2014) 58–66.
[22] I. Mohar, et al., Acetaminophen-induced liver damage in mice is associated with gender-specific adduction of peroxiredoxin-6, Redox Biol. 2 (2014) 377–387.
[23] M.R. Wieckowski, L. Wojtczak, Isolation of crude mitochondrial fraction from cells, Methods Mol. Biol. 1241 (2015) 1–8.
[24] Z.X. Liu, et al., Neutrophil depletion protects against murine acetaminophen hepatotoxicity, Hepatology 43 (6) (2006) 1220–1230.
[25] S.Y. Kim, et al., H2O2-dependent hyperoxidation of peroxiredoxin 6 (Prdx6) plays a role in cellular toxicity via up-regulation of iPLA2 activity, J. Biol. Chem. 283 (48) (2008) 33563–33568.
[26] K. Kakisaka, et al., Mechanisms of lysophosphatidylcholine-induced hepatocyte lipoapoptosis, Am. J. Physiol. Gastrointest. Liver Physiol. 302 (1) (2012) G77–G84.
[27] D. Han, et al., Regulation of drug-induced liver injury by signal transduction pathways: critical role of mitochondria, Trends Pharmacol. Sci. 34 (4) (2013) 243–253.
[28] P.C. Burcham, A.W. Harman, Acetaminophen toxicity results in site-specific mitochondrial damage in isolated mouse hepatocytes, J. Biol. Chem. 266 (8) (1991) 5049–5054.
[29] D. Han, et al., Effect of glutathione depletion on sites and topology of superoxide and hydrogen peroxide production in mitochondria, Mol. Pharmacol. 64 (5) (2003) 1136–1144.
[30] Y. Manevich, et al., Binding of peroxiredoxin 6 to substrate determines differential phospholipid hydroperoxide peroxidase and phospholipase A(2) activities, Arch. Biochem. Biophys. 485 (2) (2009) 139–149.
[31] K. Du, A. Ramachandran, H. Jaeschke, Oxidative stress during acetaminophen hepatotoxicity: sources, pathophysiological role and therapeutic potential, Redox Biol. 10 (2016) 148–156.
[32] J. Lin, et al., Comparative analysis of phase I and II enzyme activities in 5 hepatic cell lines identifies Huh-7 and HCC-T cells with the highest potential to study drug metabolism, Arch. Toxicol. 86 (1) (2012) 87–95.